



ELSEVIER

Available online at [www.sciencedirect.com](http://www.sciencedirect.com)

SCIENCE @ DIRECT®

Journal of Magnetism and Magnetic Materials 290–291 (2005) 1282–1285

**M** Journal of  
**M** magnetism  
**M** and  
magnetic  
materials[www.elsevier.com/locate/jmmm](http://www.elsevier.com/locate/jmmm)

# Texture memory effect of Nd–Fe–B during hydrogen treatment

Y. Honkura<sup>a</sup>, C. Mishima<sup>a</sup>, N. Hamada<sup>a</sup>, G. Drazic<sup>b</sup>, O. Gutfleisch<sup>c,\*</sup><sup>a</sup>*Aichi Steel Corporation, Arao-machi, Tokai-shi, Aichi-ken 476-8666, Japan*<sup>b</sup>*Jozef Stefan Institute, Jamova 39, 1001 Ljubljana, Slovenia*<sup>c</sup>*IFW Dresden, Institute for Metallic Materials, P.O. Box 270016, D-01171 Dresden, Germany*

Available online 14 December 2004

## Abstract

Highly textured magnet powder can be produced when Nd<sub>2</sub>Fe<sub>14</sub>B alloy reacts reversibly with hydrogen at high temperature (1073 K). This treatment holds promise as a production method for high-performance magnets. The appearance of anisotropy or isotropy in the magnet powder is determined by the rate of the reaction between Nd<sub>2</sub>Fe<sub>14</sub>B and hydrogen, which has been formulated in the “dynamic-hydrogenation disproportionation desorption recombination” (d-HDDR) process. The phenomena of the d-HDDR treatment are summarised in this paper including the review of the anisotropy mechanism termed here as the “texture memory effect”.

© 2004 Elsevier B.V. All rights reserved.

**Keywords:** Permanent magnet; Nd–Fe–B; HDDR; Texture; Electron microscopy

## 1. Introduction

Anisotropic Nd<sub>2</sub>Fe<sub>14</sub>B magnet powder with high performance is produced when NdFeB alloy and hydrogen react reversibly at high temperature (1073 K) [1,2]. This treatment holds promise as a production method for magnets, which will enable, e.g. the design of smaller and more economical motors [3,4]. A hydrogen treatment for magnetic hardening was first reported in 1985 [5]. The hydrogenation disproportionation desorption recombination (HDDR) process was formulated in 1990 [6,7]. This treatment was improved to the d-HDDR treatment by the authors, and the specific processing conditions for anisotropy were revealed in 1996 [8]. In 2000, an anisotropic-bonded magnet with 160 kJ m<sup>−3</sup> was commercialised [3,9] and came into wide use.

In parallel with magnet development, the inducement of texture was investigated and various anisotropy mechanisms were proposed. The suggested memory sites were, for example, non-decomposed Nd<sub>2</sub>Fe<sub>14</sub>B grains [10], Fe<sub>2</sub>B [8], localised strain [11], and Fe<sub>3</sub>B [12,13]. In the hypothesis of non-decomposed Nd<sub>2</sub>Fe<sub>14</sub>B regions, the anisotropy mechanism is constructed on the basis of the fact that anisotropy appears in the Co-added NdFeB, reported in 1990 [1]. However, this hypothesis was disagreed with because texture was also observed in ternary Nd–Fe–B, i.e. without Co [13,14]. The authors of the present paper discovered that the appearance of anisotropy or isotropy is determined by the rate of the reaction between NdFeB and hydrogen, which led to the d-HDDR process, and then proposed the Fe<sub>2</sub>B hypothesis for the anisotropy mechanism. We consider Fe<sub>3</sub>B as an insufficient orientation carrier as it is a metastable phase and can only be used under specific conditions [13]. However, the stable derivative of Fe<sub>3</sub>B is Fe<sub>2</sub>B and we observed the aligned Fe<sub>2</sub>B phase during the disproportionation step in the d-HDDR treatment [15]. In this paper, we summarise the phenomena in

\*Corresponding author. Tel.: +49 351 4659 664;  
fax: +49 351 4659 537.

E-mail address: [o.gutfleisch@ifw-dresden.de](mailto:o.gutfleisch@ifw-dresden.de) (O. Gutfleisch).

the d-HDDR treatment and the anisotropy mechanism, and then term this anisotropy mechanism as the “texture memory effect” (TME).

## 2. The d-HDDR phenomena

In the conventional HDDR treatment, which is based on the equilibrium state, the formation of fine grains can be understood, but the formation of texture and the appearance of anisotropy remained unclear. In the d-HDDR treatment, which is based on the control of the reaction rate between NdFeB and hydrogen, the specific processing conditions for anisotropy were revealed as shown in Fig. 1 (top). The maximum energy product  $(BH)_{\max}$  depends strongly on hydrogen pressure. In other words, the control of the reaction rate between NdFeB and hydrogen enables isotropy or anisotropy. The effect of Nb and Ga on  $(BH)_{\max}$  is shown by comparing with  $\text{Nd}_{12.5}\text{Fe}_{\text{bal.}}\text{B}_{6.2}$ . A  $(BH)_{\max}$  of  $343 \text{ kJ m}^{-3}$  was obtained for the  $\text{Nd}_{12.5}\text{Fe}_{\text{bal.}}\text{B}_{6.4}\text{Ga}_{0.3}\text{Nb}_{0.2}$  alloy. The effect of Co on  $(BH)_{\max}$  on the reaction kinetics is shown in Fig. 1 (bottom). As the quantity of Co increases, the hydrogen pressure needs to be increased in order to maximise  $(BH)_{\max}$ . Consistent with Refs. [16,17], it is then

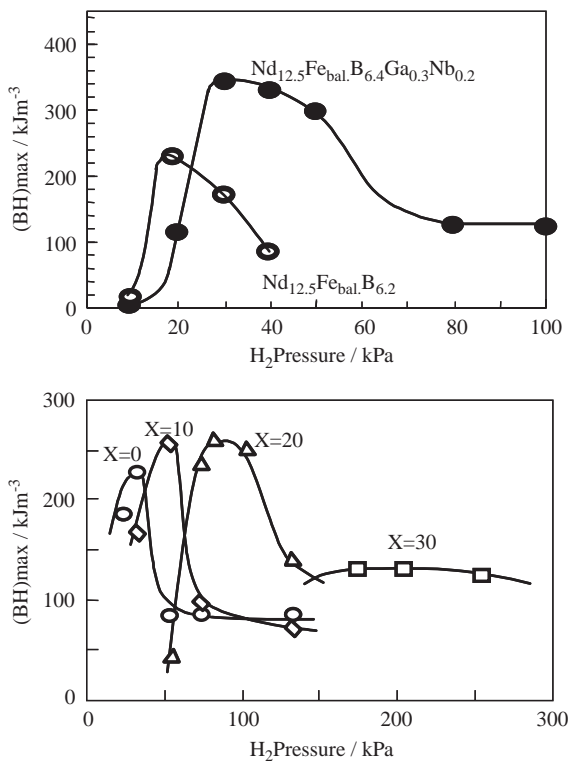


Fig. 1. Effect of hydrogen pressure on  $(BH)_{\max}$  at 1093 K in (top)  $\text{Nd}_{12.5}\text{Fe}_{\text{bal.}}\text{B}_{6.2}$  and  $\text{Nd}_{12.5}\text{Fe}_{\text{bal.}}\text{B}_{6.4}\text{Ga}_{0.3}\text{Nb}_{0.2}$  and (bottom) in  $\text{Nd}_{12.5}\text{Fe}_{\text{bal.}}\text{B}_{6.0}\text{Ga}_{1.0}\text{Co}_X$ .

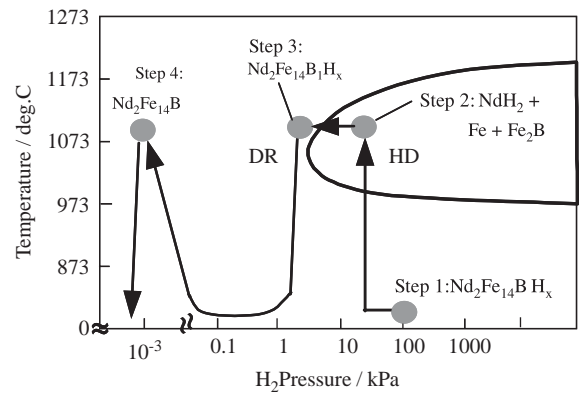


Fig. 2. The d-HDDR process in the  $\text{Nd}_2\text{Fe}_{14}\text{B}$ -H phase diagram.

found that Co is the element, which lowers the reaction rate. In the past, Co was considered an essential element for anisotropy, and it can be assumed that the experiments were performed at atmospheric pressure. Moreover, the effect of various additive elements was studied, and it was found that Ga and Nb are effective elements for coercivity and anisotropy, respectively.

In the HDDR reaction, the process for anisotropy was formulated as the d-HDDR treatment. In order to achieve industrial products, the d-HDDR treatment consists of 4 steps, as shown in Fig. 2. In step 1, hydrogen is sufficiently absorbed into  $\text{Nd}_2\text{Fe}_{14}\text{B}$  without disproportionation. In step 2,  $\text{Nd}_2\text{Fe}_{14}\text{BH}_x$  is slowly disproportionated into 3 phases. In step 3, the 3 phases are recombined into  $\text{Nd}_2\text{Fe}_{14}\text{BH}_x$ . Finally, in step 4, residual hydrogen is removed from  $\text{Nd}_2\text{Fe}_{14}\text{BH}_x$ . Steps 2 and 3 are the key processes for the appearance of anisotropy. Steps 1 and 4 are just the absorption process and desorption process of hydrogen.

## 3. Hypothesis for anisotropy mechanism

First, the structural change during hydrogen treatment is such that, in the hydrogenation disproportionation process, the lamellar structure is formed at the early stage (compare Figs. 3 (left) and 4), and the structure changes into a spherical morphology (Fig. 3 (right)) as reaction time increases. In the desorption recombination process, a rim phase of  $\text{Nd}_2\text{Fe}_{14}\text{B}$ -type appears around the Nd-hydride phase at the early stage, and finally the recrystallisation to  $\text{Nd}_2\text{Fe}_{14}\text{B}$  is completed. Looking at the crystal structures, tetragonal  $\text{Nd}_2\text{Fe}_{14}\text{B}$  decomposes into 3 phases, which are cubic  $\text{NdH}_2$ , cubic Fe and tetragonal  $\text{Fe}_2\text{B}$  in the disproportionation process. In step 3 of the process, tetragonal  $\text{Nd}_2\text{Fe}_{14}\text{B}$  is recrystallised from 3 phases. Within the 3 phases, only  $\text{Fe}_2\text{B}$  has an anisotropic

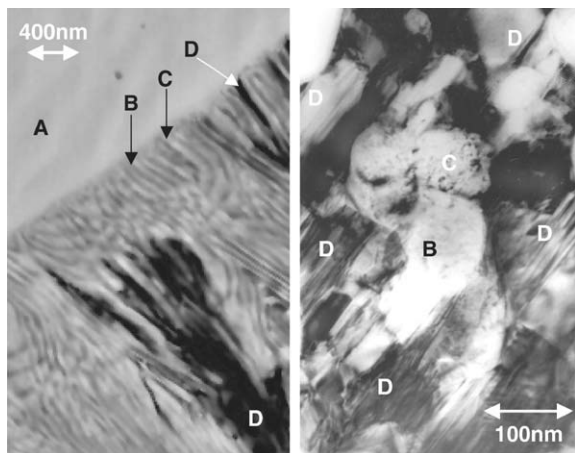


Fig. 3. (left) SEM micrograph in the backscattered mode showing the reaction front upon disproportionation; (right) TEM bright field image showing well-aligned  $\text{Fe}_2\text{B}$  grains within the disproportionated structure (A— $\text{Nd}_2\text{Fe}_{14}\text{B}$ , B—Fe/Fe(B), C— $\text{NdH}_2$  and D— $\text{Fe}_2\text{B}$ ).

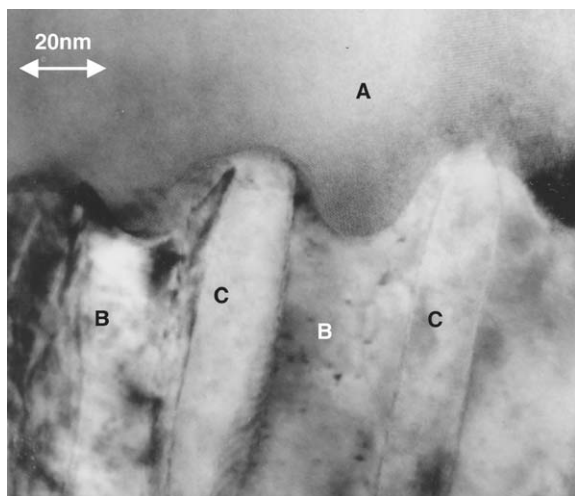


Fig. 4. TEM bright field image showing the reaction front upon disproportionation in more detail (A— $\text{Nd}_2\text{Fe}_{14}\text{B}$ , B—Fe/Fe(B), and C— $\text{NdH}_2$ ).

crystal structure indicating that the  $\text{Fe}_2\text{B}$  phase could be crucial for the memory effect of anisotropy. This hypothesis is shown schematically in Fig. 5. After decomposition, tetragonal  $\text{Fe}_2\text{B}$  phases precipitates along to tetragonal  $\text{Nd}_2\text{Fe}_{14}\text{B}$ , and the  $\text{Fe}_2\text{B}$  crystallites keep the crystal orientation of  $\text{Nd}_2\text{Fe}_{14}\text{B}$  during phase transformation. Subsequently, fine-grained  $\text{Nd}_2\text{Fe}_{14}\text{B}$  phases precipitates in step 3. We assume that the degree of alignment, that is, the fluctuation of  $\text{Fe}_2\text{B}$ , depends on the reaction rate.  $\text{Fe}_2\text{B}$  memorises the direction of  $\text{Nd}_2\text{Fe}_{14}\text{B}$  sufficiently if the reaction rate between hydrogen and  $\text{NdFeB}$  is low, and as a result, recombined  $\text{Nd}_2\text{Fe}_{14}\text{B}$  will be anisotropic.  $\text{Fe}_2\text{B}$  precipitates at

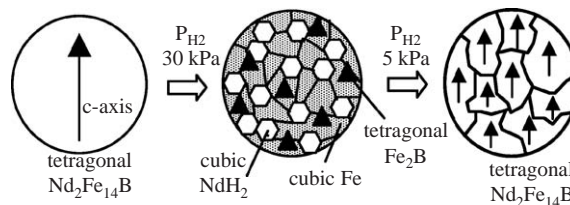


Fig. 5. Schematic structural changes with  $\text{Fe}_2\text{B}$  as the hypothetical orientation memory site: (left) before d-HDDR, (middle) disproportionated structure with aligned  $\text{Fe}_2\text{B}$  and (right) fine grained, textured material after d-HDDR.

random if the reaction is higher due to a higher hydrogen partial pressure, and  $\text{Nd}_2\text{Fe}_{14}\text{B}$  will be isotropic.

#### 4. Structural changes during d-HDDR

Experimental evidence for the  $\text{Fe}_2\text{B}$  hypothesis was obtained using scanning and transmission electron microscopy (SEM, TEM). The conditions of d-HDDR treatment are 1093 K for 3 h in hydrogen pressure of 30 kPa for disproportionation (step 2), and 5 kPa upon recombination (step 3). For details of the experiment, please refer to Ref. [15]. Fig. 4 shows the reaction front moving from the parent phase (A) to the disproportionated phases (B,C,D) in more detail. A lamellar structure of  $\text{NdH}_2$  and Fe is observed at the wave-shaped interface. Electron energy loss spectroscopy (EELS) shows that some boron is found in the Fe, indicating a possible initial oversaturation of boron in Fe. In the progress of the reaction, the Fe(B) phase is transformed into  $\text{Fe}_2\text{B}$  and Fe, and well-aligned  $\text{Fe}_2\text{B}$  precipitates. The lamella structure is the key for precipitated and well-aligned  $\text{Fe}_2\text{B}$ . There must be uni-axial stress along the interface because of the lamellar structure. Well-aligned tetragonal  $\text{Fe}_2\text{B}$  may precipitate along the uni-axial stress in order to relieve the stress. Fig. 3 (right) shows the completion of disproportionation into  $\text{NdH}_2$ , Fe and  $\text{Fe}_2\text{B}$ .  $\text{Fe}_2\text{B}$  grains have stacking faults, indicated by the hatched lines in the TEM bright field image. Stacking faults could be induced during the rapid cooling. The hatched lines are all well aligned in one direction and more detailed conventional beam electron diffraction (CBED) analysis reveals that  $\text{Fe}_2\text{B}$  crystallites are aligned within  $20^\circ$  during all processing steps. Therefore, it is thought that this well-aligned  $\text{Fe}_2\text{B}$  is a memory phase for anisotropy after recombination. We term this mechanism “texture memory effect (TME)”.

#### 5. Projections

In 1997, bonded  $\text{NdFeB}$  magnets with  $136 \text{ kJ m}^{-3}$  were first commercialised into market, and in 2002, the

performance of bonded magnets increased up to  $200 \text{ kJ m}^{-3}$ . In the laboratory, a bonded magnet with  $216 \text{ kJ m}^{-3}$  has been produced [18]. The accomplished detailed knowledge of the “texture memory effect (TME)” should enable the realisation of further improved magnetic properties. In the near future, an anisotropic bonded NdFeB magnet with about  $240 \text{ kJ m}^{-3}$  could be produced on an industrial scale.

## References

- [1] T. Takeshita, N. Nakayama, Proceedings of the 11th International Workshop on RE Magnets and their Applications, Pittsburgh, 1990, p. 49.
- [2] O. Gutfleisch, I.R. Harris, Proceedings of the 15th International Workshop on RE Magnets and their Applications, 1998, p. 487.
- [3] Y. Honkura, Proceedings of the 7th International Workshop on RE Magnets and their Applications, Delaware, 2002, p. 52.
- [4] Y. Hayashi, H. Mitarai, Y. Honkura, IEEE Trans. Magn. 39 (2003) 2893.
- [5] Y. Inoue, N. Imaizumi, Tokukaisho 62-23903 (Japanese patent).
- [6] T. Takeshita, R. Nakayama, Proceedings of the 10th International Workshop on RE Magnets and their Applications, 1989, p. 551.
- [7] P.J. McGuiness, X.J. Zhang, X.J. Yin, I.R. Harris, J. Less-Common Metals 158 (1990) 379.
- [8] H. Honkura, C. Mishima, H. Mitarai, Tokaihei 10-135019 (Japanese patent).
- [9] C. Mishima, N. Hamada, H. Mitarai, Y. Honkura, IEEE Trans. Magn. 37 (2001) 2467.
- [10] M. Uehara, H. Tomizawa, S. Hirosawa, T. Tomida, Y. Maehara, IEEE Trans. Magn. 29 (1993) 2770.
- [11] H. Nakamura, K. Kato, D. Book, S. Sugimoto, M. Okada, M. Homma, J. Magn. Soc. Jpn. 23 (1999) 300.
- [12] T. Tomida, N. Sano, K. Hanafusa, H. Taomizawa, S. Hirosawa, Acta Mater. 47 (1999) 875.
- [13] O. Gutfleisch, B. Gebel, N. Mattern, J. Magn. Magn. Mater. 210 (2000) 5.
- [14] H. Nakamura, R. Suefuji, S. Sugimoto, M. Okada, M. Homma, J. Appl. Phys. 76 (1994) 6828.
- [15] O. Gutfleisch, K. Khlopkov, A. Teresiak, K.H. Muller, G. Drazic, C. Mishima, Y. Honkura, IEEE Trans. Magn. 39 (2003) 2926.
- [16] A. Fujita, I.R. Harris, IEEE Trans. Magn. 30 (1994) 860.
- [17] S. Sugimoto, O. Gutfleisch, I.R. Harris, J. Alloys Compound. 260 (1997) 284.
- [18] N. Hamada, C. Mishima, H. Mitarai, Y. Honkura, IEEE Trans. Magn. 39 (2003) 2953.